



Title	Introduction of the harmonic distortion determining factor and its application to evaluating real time PWM inverters
Author(s)	Fukuda, S.; Iwaji, K.
Citation	IEEE Transactions on Industry Applications, 31(1), 149-154 https://doi.org/10.1109/28.363037
Issue Date	1995
Doc URL	http://hdl.handle.net/2115/6076
Rights	© 1995 IEEE. Personal use of this material is permitted. However, permission to reprint/republish this material for advertising or promotional purposes or for creating new collective works for resale or redistribution to servers or lists, or to reuse any copyrighted component of this work in other works must be obtained from the IEEE. " IEEE, IEEE Transactions on Industry Applications, 1995, Volume: 31 , Issue: 1 , page(s): 149 - 154
Type	article
File Information	ITIA31-1.pdf



[Instructions for use](#)

Introduction of the Harmonic Distortion Determining Factor and Its Application to Evaluating Real Time PWM Inverters

Shoji Fukuda, *Member, IEEE*, and Yoshitaka Iwaji

Abstract—Frequency spectra of inverter output currents are one of the important factors in order to evaluate PWM methods. These spectra are, however, influenced not only by the PWM method itself but by the operating conditions of the inverter such as the switching frequency or load parameters. The harmonic distortion determining factor (HDDF) is considered to be a common quality index that represents the intrinsic spectral property of individual PWM methods. As it has a close relation to RMS values of the harmonic current or torque ripples of driven motors and, further, it is almost independent of the operating conditions, HDDF is quite useful for evaluating PWM methods. In this paper three typical analog PWM methods and four digital PWM methods are compared and evaluated based on HDDF values.

I. INTRODUCTION

MANY real time PWM methods for inverter control have been proposed [1]–[4]. The spectral property of the inverter output current is one of the important factors used to evaluate a PWM method. Evaluation of PWM methods is, however, not easy because the frequency spectra of the inverter current are greatly influenced by the switching frequency and load parameters of the inverter. For instance, if the switching frequency is very high or the load inductance is very large compared to the load resistance, the current spectra will be excellent irrespective of the PWM method.

Therefore, a common quality index which is independent of the inverter operating conditions such as the switching frequency and load parameters is desirable for evaluating a selected PWM method. The harmonic distortion determining factor (HDDF), a function of the modulation index of the inverter, is one candidate for such a quality index.

HDDF is also useful for predicting the harmonic properties of PWM inverters. For instance, the harmonic characteristics such as the spectra of motor current harmonics or torque ripples in the case of ac drives are usually obtained by Fourier transformation or simulation. However, if HDDF values for individual PWM's are known, the approximate

harmonic characteristics are easily calculated by using the HDDF values.

In this paper, the basic idea and physical meaning of HDDF is first described by means of a simple example, a dc/dc down converter. Then the idea of HDDF is expanded to include three-phase PWM inverters. Next, the relation of HDDF to the RMS value of motor current harmonics or torque ripples in the case of ac drives, and the relation of HDDF to the RMS value of ac side harmonic current or dc side harmonic voltage in the case of rectifier operation are described. In short, HDDF is a normalized representation of the RMS distortion current, which has been used in [5] for comparing two PWM's in the case of an IM drive, the sine PWM and the space vector PWM. Here, however, two kind HDDF's, *d*-axis HDDF and total HDDF, are introduced and used. Finally HDDF curves under variable output voltage conditions are illustrated for typical real time PWM's, three analog PWM's and four digital PWM's, and evaluations of these PWM methods based on the HDDF values are given.

II. BASIC IDEA OF HDDF

To clarify the basic idea of HDDF, consider the dc/dc down converter shown in Fig. 1. We know empirically the following facts concerning RMS value of the ac or harmonic component of the load current, I_h :

- 1) I_h is directly proportional to the dc supply voltage V_{dc} .
- 2) I_h is almost inversely proportional to the inductance L .
- 3) I_h is almost inversely proportional to the switching or chopping frequency ω_s .
- 4) I_h is almost independent of the resistance R .
- 5) I_h is almost independent of the dc load current I_{dc} .

From these facts, the ac current will be approximately represented by

$$I_h = \frac{V_{dc}}{\omega_s L} P(M) \quad (1)$$

where P , which is only a function of the duty ratio, $M = t_{on}/T$, is called the harmonic distortion determining factor of the dc/dc converter. If $\omega_s L \gg R$, (1) gives us a good approximation of the RMS value of the load harmonic current.

Let us derive (1). The switching function, S , of the dc/dc converter in Fig. 1 is defined as:

- $$\begin{aligned} S &= 1 \text{ when the transistor is ON,} \\ S &= 0 \text{ when the transistor is OFF.} \end{aligned}$$

Paper IPCSD 94-59, approved by the Industrial Power Converter Committee of the IEEE Industrial Applications Society for presentation at the 1993 Industrial Applications Society Annual Meeting, Toronto, Ontario, Canada, October 3-8, and the IEEJ Technical Meeting on Semiconductor Power Converter, Naha, Okinawa, Japan, Oct. 25-26, 1994. Manuscript released for publication July 21, 1994.

S. Fukuda is with the Department of Electrical Engineering, Hokkaido University, Sapporo, 060 Japan.

Y. Iwaji is with Hitachi Research Laboratory, Hitachi Ltd., Ibaraki, 319-12 Japan.

IEEE Log Number 9406604.

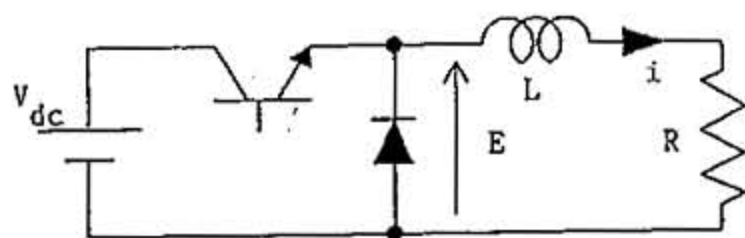


Fig. 1. A dc/dc step down converter.

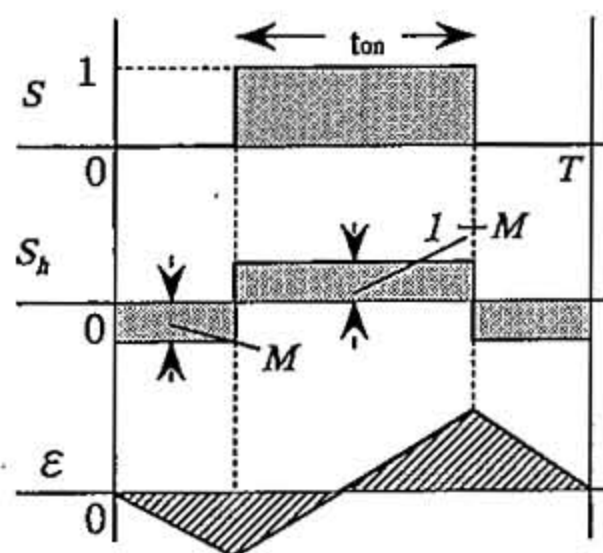


Fig. 2. Normalized voltage pulses and resulting harmonic current within one chopping period.

If the chopping frequency, ω_s , is high enough, then $\omega_s L \gg R$, and the ac load current i_h will be determined by:

$$L \frac{d}{dt} i_h = E - MV_{dc} = V_{dc}(S - M) = V_{dc} S_h \quad (2)$$

where S_h denotes the ac or harmonic component of SF. Fig. 2 shows the waveforms of S and S_h for one chopping interval, T . Solving (2) we have

$$i_h = \frac{V_{dc}}{L} \epsilon, \quad \epsilon = \int S_h dt \quad (3)$$

where ϵ is the normalized ac component of the load current, and its waveform is shown in Fig. 2.

Now define HDDF of the dc/dc converter as:

$$P = \omega_s \sqrt{\frac{1}{T} \int_0^T \epsilon^2 dt} = \frac{\pi(1-M)M}{\sqrt{3}} \quad (4)$$

where T denotes the chopping interval. Then the RMS of i_h is given by (1). The ac current I_h for any M values is easily calculated if P and the operating conditions, ω_s , L and V_{dc} , are given. It is noted that P is independent of the operating parameters of the dc/dc converter.

III. HDDF FOR THREE PHASE PWM INVERTERS

Here the idea of HDDF is expanded to include a three-phase inverter. Consider the PWM voltage source inverter shown in Fig. 3 which is supplying ac power to an inductive load.

A. Switching Function

The switching function (SF) of the inverter for phase "a" is defined as:

$S_a = 1$ when the upper arm switch S_{a+} is ON,
 $S_a = -1$ when the lower arm switch S_{a-} is ON.

SF's for phase "b" and "c" are also defined similarly. The output potentials of the inverter are obtained by multiplying SF by the dc source voltage V_{dc} .

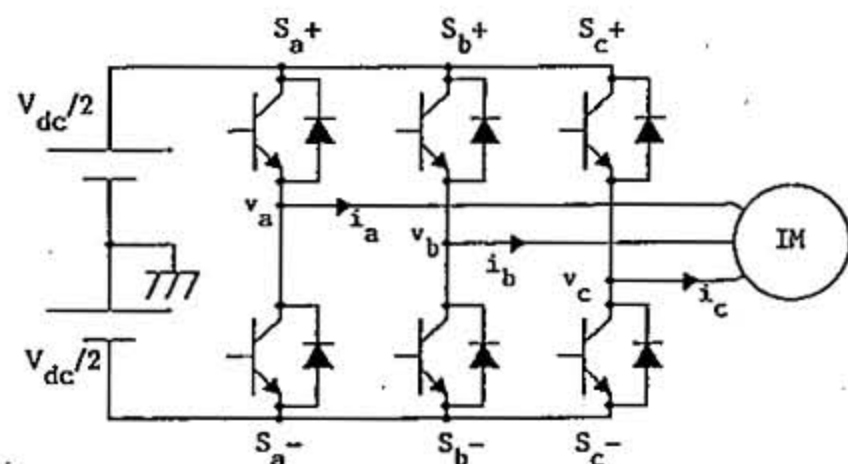


Fig. 3. A voltage source inverter.

B. Transformation of the SF into the d - q Coordinate

S_a, S_b, S_c in the real axis are transformed into S_d and S_q in the d - q axis, which is rotating at an angular inverter output frequency, ω . The fundamental component of the inverter output will then be represented by a dc component. Thus, situations similar to those of the dc/dc converter are obtained. The q axis is selected to make its dc component equal to zero. Let S_{dh} and S_{qh} be the ac components of S_d and S_q , respectively. S_{dh} and S_{qh} correspond to the harmonic voltages of the inverter output.

C. Definition of HDDF

If the switching frequency, ω_s , is high enough, then $\omega_s L \gg R$, and d -axis harmonic current, i_{dh} , will be given by:

$$i_{dh} = \frac{V_{dc}}{L} \epsilon_d, \quad \epsilon_d = \int S_{dh} dt. \quad (5)$$

Then, HDDF's in the d and q axes are defined by expressions similar to (4):

$$\left. \begin{aligned} P_d &= \frac{\omega_s}{\sqrt{2}} \sqrt{\frac{1}{T} \int_0^T \epsilon_d^2 dt}, & P_q &= \frac{\omega_s}{\sqrt{2}} \sqrt{\frac{1}{T} \int_0^T \epsilon_q^2 dt} \\ P &= \sqrt{P_d^2 + P_q^2} \end{aligned} \right\} \quad (6)$$

where T denotes one-sixth of an inverter output period. As the switching function is determined in relation to the modulation index, M , P_d and P_q are primarily functions of M . It has been confirmed that neither P_d nor P_q depends on the frequency ratio, ω_s/ω , if ω_s/ω is larger than 40.

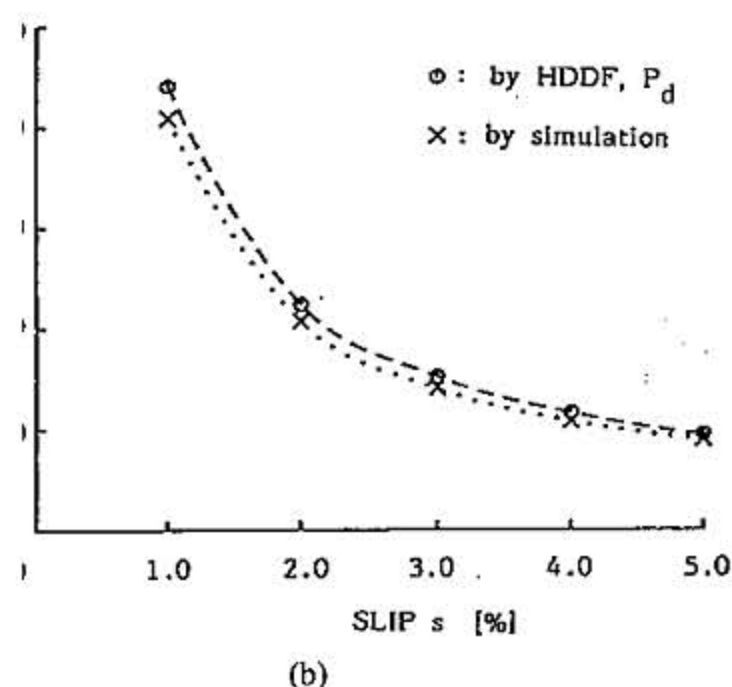
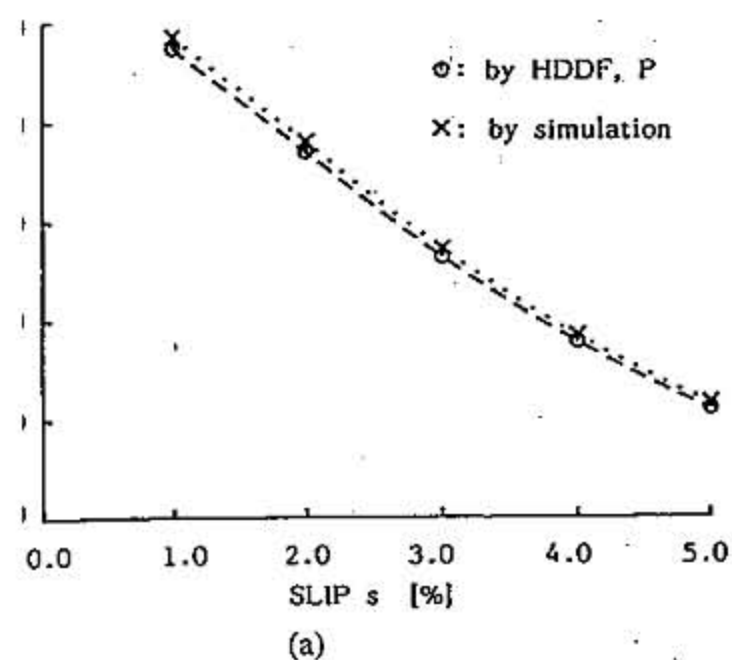
IV. RELATION BETWEEN HDDF AND INVERTER PERFORMANCE

A. Induction Motor Drives

The prediction of harmonic characteristics of ac drives such as the RMS of motor current or torque pulsations is easily done by using HDDF. In the case of induction motor drives, we have shown [6], [7] that the RMS values of the input harmonic current, I_h , and torque ripples, T_h of the driven motor are approximately obtained by

$$I_h = \sqrt{\sum_{k=2}^{\infty} I_k^2} = \frac{V_{dc}}{2\omega_s l} P, \quad T_h = \sqrt{\sum_{k=1}^{\infty} T_k^2} = \frac{MV_{dc}^2}{2\sqrt{2}\omega_s \omega l} P_d \quad (7)$$

where l denotes the leakage inductance of the motor per phase, and I_k and T_k denote the RMS values of the k -th harmonic current and the k -th harmonic torque, respectively. I_h and T_h values obtained by simulation and by HDDF are compared



son of RMS values in ac drives obtained by simulation and
otor current harmonics. (b) Torque ripples.

ere the original sine-triangular PWM is used;
ratio is $\omega_s/\omega = 36$ and the modulation index
stant. Definitions of THD are:

$$\text{THD}_i = \frac{I_h}{I_1}, \quad \text{THD}_t = \frac{T_h}{T_0}$$

T_0 denote the RMS values of the motor funda-
t and the motor average torque, respectively. The
an example has the following ratings: 0.75 [kW],
50 [Hz], $f_s = 1.8$ [kHz] and $V_{dc} = 141$ [V]
r constants; $L_1 = L_2 = 15.1$ [mH], $M_m = 146$
l [Ω], and $R_2 = 1.3$ [Ω]. It is seen that both the
ed by simulation and by HDDF are very close

Age Source Rectifiers

feature of a PWM voltage source rectifier is
it dc voltage can be controlled while keeping
ic input current. In this situation, the induction
source, V_{dc} in Fig. 3 are replaced by an ac
d the parallel combination of a filter capacitor,
luctive load, $R_1 + L_1$, respectively. Power flow
om the ac side to the dc side. We have shown [8],
of the input harmonic current, I_h , and RMS of
monic voltage, V_h , are approximately given by

$$I_h = \frac{V_{dc0}}{\omega_s L} P, \quad V_h = \frac{I_{d0}}{\omega_s C} P_d \quad (8)$$

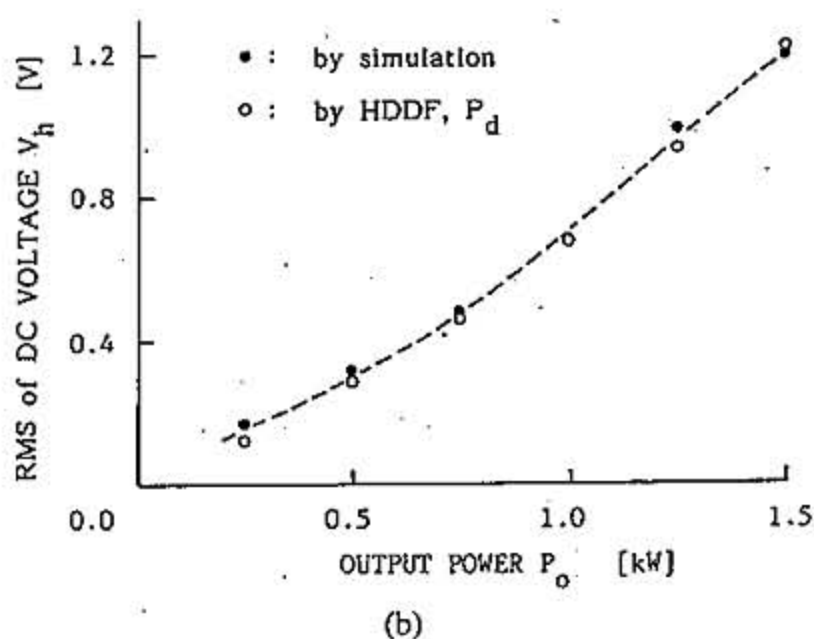
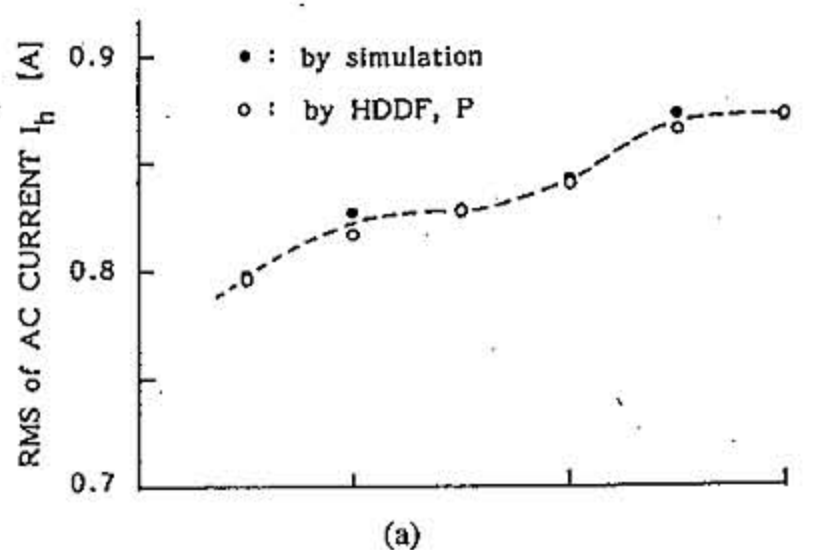


Fig. 5. Comparison of RMS values in rectifier operation obtained by simulation and by HDDF. (a) AC current harmonics, (b) DC voltage harmonics.

where V_{dc0} and I_{d0} denote the average dc output voltage and the d -axis current, respectively; L and C denote the inductance of the ac reactor and capacitance of the dc capacitor, respectively. The RMS values of input harmonic current, I_h , and output harmonic voltage, V_h , obtained by simulation and by HDDF are compared in Fig. 5, where the original sine-triangular PWM method is used and the inverter operating conditions are $E = 100$ [V], $f = 50$ [Hz], $f_s = 1.8$ [kHz], $L = 5$ [mH], $R = 1$ [Ω], $C = 330$ [μ F], $V_{dc0} = 160$ [V], $\omega_s/\omega = 36$ and $L_1 = 1.6$ [mH]. To vary the output power, R_1 is changed while maintaining PF at unity and keeping V_{dc} constant. The modulation index M and phase angle δ are simultaneously adjusted over the range, $M = 0.862$ to 0.765 and $\delta = 2.37$ to 19.5 [$^\circ$], respectively and correspond to the power range $P_0 = 0.25$ to 1.5 [kW]. I_h and V_h are shown in terms of P_0 rather than in terms of M because the range over which M varies is too small. Both curves obtained by simulation and by HDDF are very close to each other.

Figs. 4 and 5 clearly show that once HDDF curves of the selected PWM method have been calculated, the harmonic characteristics of PWM inverter or PWM rectifier systems can be easily predicted without simulation.

V. APPLICATION OF HDDF TO EVALUATE REAL TIME PWM METHODS

A. Analog PWM

Here, HDDF curves of three typical real time analog PWM methods are compared and evaluated. They are the original sine-triangular PWM (SPWM) [1] shown in Fig. 6, har-

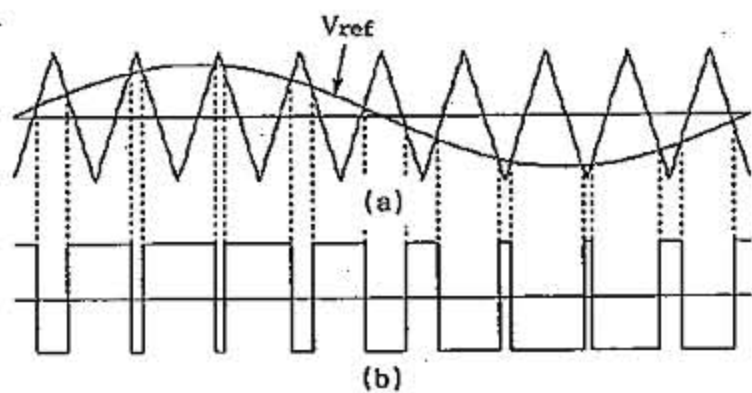


Fig. 6. Original sine PWM.

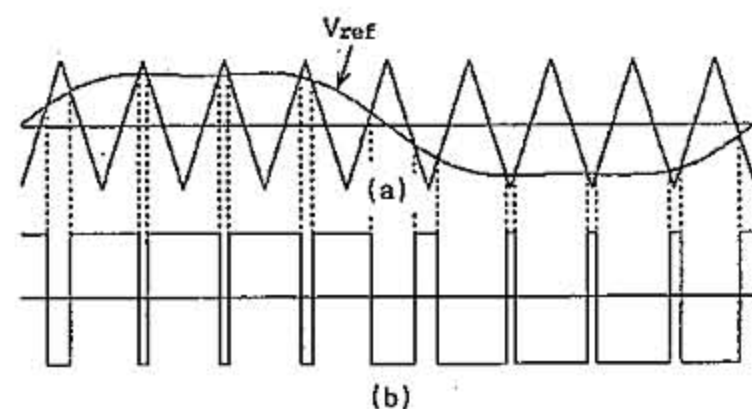


Fig. 7. Third-harmonic injected PWM.

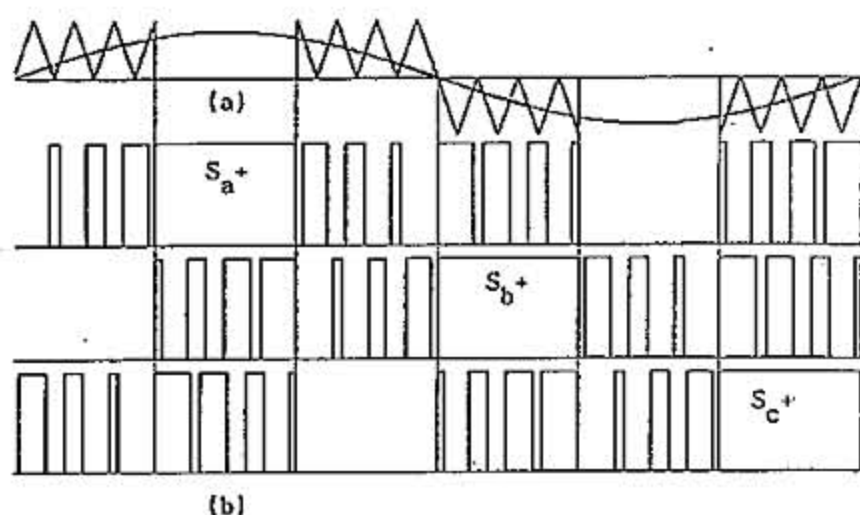
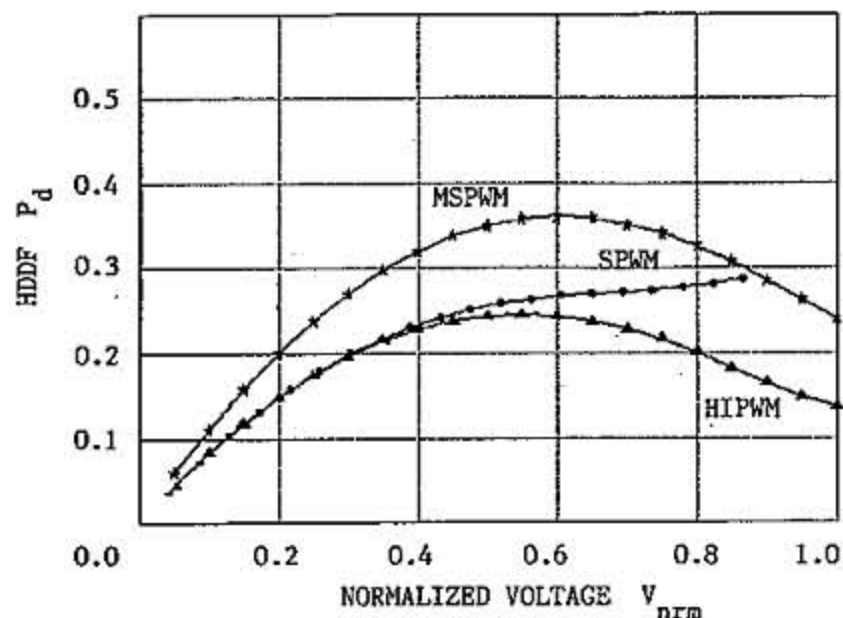
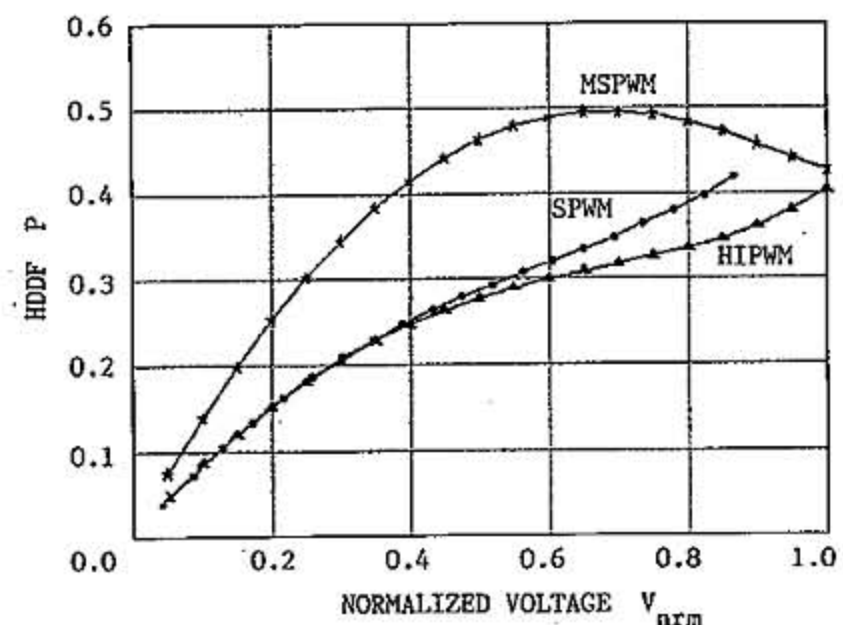


Fig. 8. Modified sine PWM. (a) MSPWM scheme. (b) Transistor gating signals.

monic injection PWM [2] (HIPWM), and modified sine PWM (MSPWM) [3]. HIPWM is derived from SPWM through the addition of the 17% third-harmonic component to the original sine reference waveform as shown in Fig. 7, where V_{ref} denotes the reference. The aim of injecting the third harmonic is to increase the maximum fundamental output voltage. Figs. 6 and 7, (b) shows the output potential for one phase. MSPWM defines the output on a line-to-line basis. Only the first and last 60° intervals (per half-cycles) of the ac waveform are directly defined through intersections of respective sine and triangular waves as shown in Fig. 8, where (b) shows gating signals for each phase switch. The maximum output voltage by SPWM is 86.7% of that by HIPWM and MSPWM.

HDDF curves under variable voltage conditions are shown in Figs. 9 and 10, where the inverter output and carrier frequencies are $f = 50$ [Hz] and $f_s = 2.25$ [kHz], respectively. The output voltage V_{nrm} (normalized by V_{dc}) for different PWM strategies and equivalent modulation index M differ. Thus, for comparison purposes, it is more instructive to graph HDDF as a function of V_{nrm} rather than the modulation index M . From these figures, the following observations can be made:

Fig. 9. Comparison of HDDF in the d -axis, P_d , for analog PWM's.Fig. 10. Comparison of HDDF, P , for analog PWM's.

- * SPWM and HIPWM show similar curves, but MSPWM is different. This stems from the different approach taken in creating the pulses.
- * P_q curves (not shown in the paper) of SPWM and HIPWM are almost identical.
- * Of the two similar methods, HIPWM is superior to SPWM, especially in the high output voltage region.
- * MSPWM has a higher maximum voltage than SPWM, but its characteristics are poorer except for the restricted high voltage region, $V_{nrm} > 0.8$.

In ac drives, suppression of torque ripples is important because of noise and vibration problems. From this point of view, HIPWM has an advantage over the others, especially in the high-speed region. HIPWM is also better in rectifier operation because it exhibits fewer dc voltage ripples than the others. As for the RMS of the harmonic current, there is not much difference between SPWM and HIPWM, but HIPWM is slightly better. On the whole, HIPWM is the best choice among the three.

B. Digital PWM [4]

Instantaneous space vector representation is employed to treat three-phase quantity as a whole. The instantaneous voltage vector is defined by

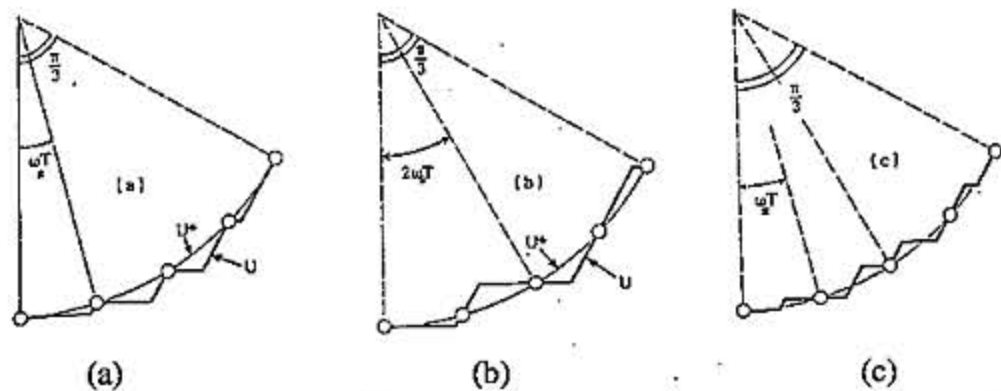


Fig. 11. Digital PWM's. (a) DPWM-A, (b) DPWM-C, and (c) DPWM-D.

$$\begin{aligned} \mathbf{V}_n &= \frac{V_{dc}}{2} (S_a + \alpha S_b + \alpha^2 S_c), \quad \text{where } \alpha = \exp\left(j\frac{2\pi}{3}\right) \\ &= V_{dc} \exp\left\{j(n-1)\frac{2\pi}{3}\right\} \quad \text{for } n = 1, \dots, 6 \\ &= 0 \quad \text{for } n = 0 \text{ or } 7 \end{aligned} \quad (9)$$

where S_a, S_b and S_c are the switching functions for each phase. The inverter can produce eight voltage vectors, $V_n, n = 0, 1, \dots, 7$, where V_0 and V_7 are so-called zero vectors. Consider the time-integral function of the inverter output vector as:

$$\mathbf{U} = \int \mathbf{V}_n dt + \mathbf{U}_0. \quad (10)$$

The reference vector U^* , which is derived from the purely sinusoidal three phase output voltage, will be given by

$$\mathbf{U}^* = -j \frac{\sqrt{3} V_{dc} M}{2\omega} \exp(j\omega t) \quad (11)$$

where M and ω denote the modulation index and output frequency of the inverter, respectively. The U^* locus represents a perfect circle.

The PWM pattern is determined at every sampling interval so that U may follow the U^* locus as closely as possible. We call this means of creating pulses the quasi-circular-locus method (QCLM) and have proposed four PWM methods based on QCLM [7]. Here, HDDF curves of the four real time digital PWM's are compared and evaluated. They are the digital PWM of type-A (DPWM-A) to digital PWM of type-D (DPWM-D). With DPWM-A, vector U moves along U^* only from outside the reference circle as shown in Fig. 11(a), where "O" shows that a zero-vector is used. With DPWM-B, U moves only from the inside the reference circle. With DPWM-C, U tracks U^* from the inside at one sampling interval, and then from the outside at the next sampling interval, alternating as shown in Fig. 11(b). The switching functions for each phase and selected voltage vectors for two sampling intervals are shown in Fig. 12, where the pulse widths for the phase angle $0 < \phi < \pi/3$ are given by:

$$\left. \begin{aligned} \alpha_1 &= MT \cos\left(\phi - \frac{\pi}{6}\right), \quad \alpha_2 = MT \cos\left(\phi + \frac{\pi}{6}\right) \\ \beta &= \frac{T - \alpha_1}{2} \end{aligned} \right\}. \quad (12)$$

With DPWM-D, U traces U^* from the inside, and then from the outside alternately at every sampling interval as shown in Fig. 11(c).

HDDF curves under variable voltage conditions are shown in Figs. 13 and 14, where the inverter output and sampling

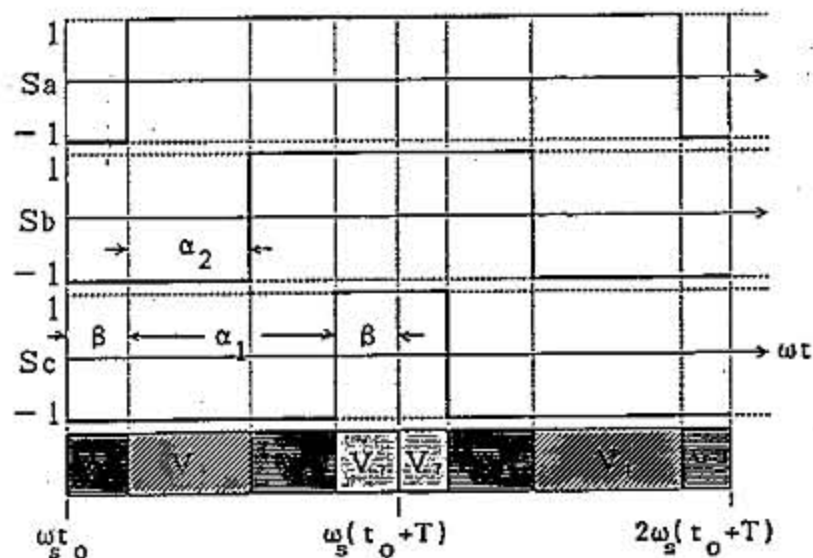
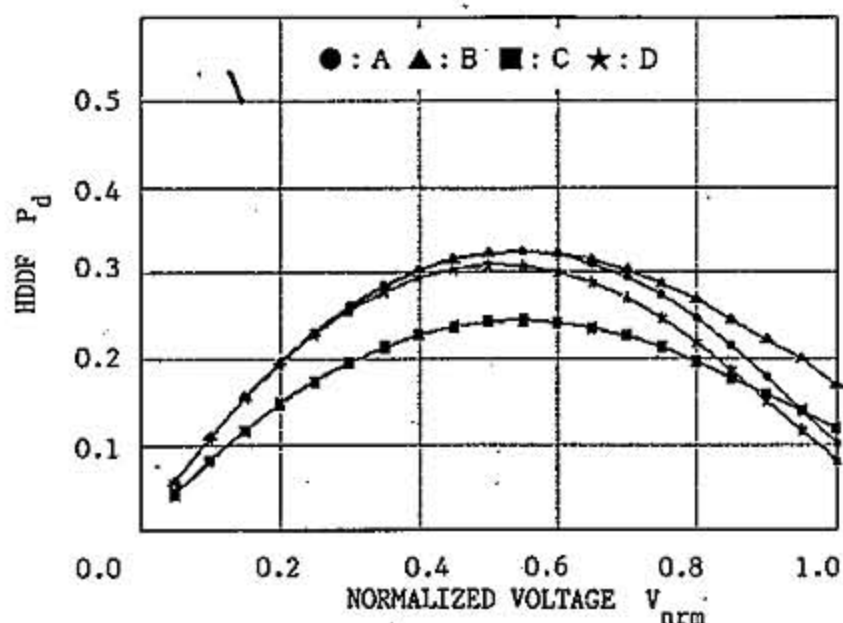
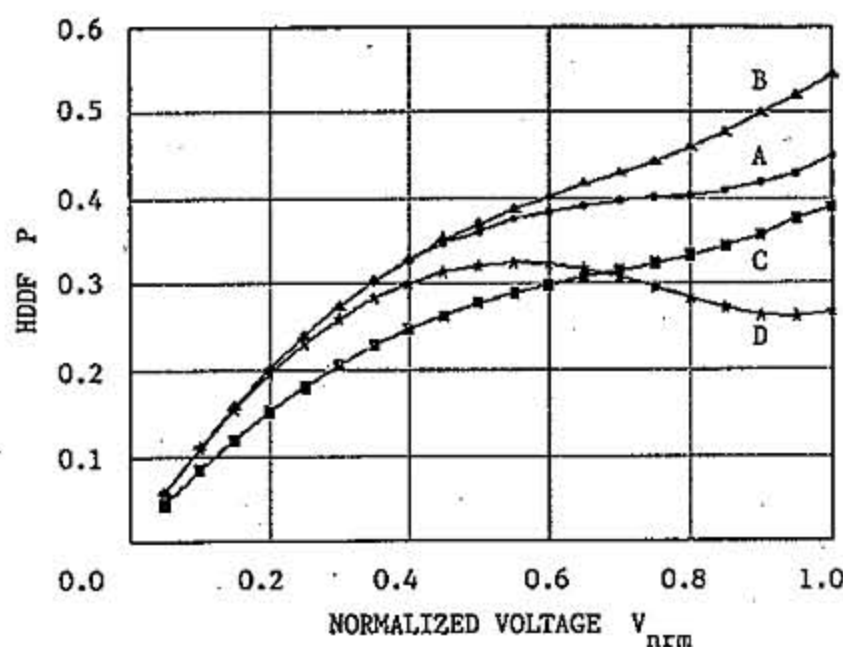


Fig. 12. Switching functions for each phase and voltage vectors used with DPWM-C for two sampling intervals.


 Fig. 13. Comparison of HDDF in the d -axis, P_d , for digital PWM's.

 Fig. 14. Comparison of HDDF, P , for digital PWM's.

frequencies are $f = 50$ [Hz] and $f_s = 1.8$ [kHz], respectively. From these figures, the following can be observed:

- * DPWM-A and -B provide similar HDDF curves, but DPWM-A is slightly better.
- * DPWM-C and D are superior to DPWM-A and B.
- * DPWM-D has an advantage over DPWM-C only in the high voltage region, $V_{nrm} > 0.7$ for P or $V_{nrm} > 0.9$ for P_d .
- * If considered on the whole, DPWM-C has the best characteristics of the four.

Therefore, for ac drives, DPWM-C is superior to the others because it produces the fewest torque ripples among the four

methods. As for the RMS of the harmonic current, DPWM-C is best in the voltage range $V_{\text{norm}} < 0.7$ but DPWM-D is the best in the range $V_{\text{norm}} > 0.7$. DPWM-A and B are poor.

If analog PWM's and digital PWM's are compared, the following can be observed:

- * Digital PWM's provide lower P_d curves than analog PWM's in the high voltage region. Therefore, digital PWM's have an advantage for AC drive applications over analog ones in the same region.
- * DPWM-C and HIPWM have almost identical HDDF curves. Thus DPWM-C is a digital alternative of HIPWM.
- * If an analog PWM is adopted, HIPWM would be the best choice, and if a digital PWM is adopted, method C would be the best choice.

C. Normalization of Switching Frequency

As for the analog PWM's, each phase has one switch-transition at every sampling time because each phase is controlled independently. As for the digital PWM's, however, the average switching number depends on the individual method because the three phases are not treated independently. Therefore, normalization of switching frequency is necessary to evaluate PWM methods. The average switching frequency, f_{sw} of each method is:

$$\begin{aligned} f_{\text{sw}} &= f_c && \text{for the analog PWM's,} \\ f_{\text{sw}} &= (2/3)f_s && \text{for DPWM-A, DPWM-B and DPWM-D, and} \\ f_{\text{sw}} &= (1/2)f_s && \text{for DPWM-C.} \end{aligned}$$

where f_c and f_s are the carrier and sampling frequencies, respectively. The HDDF curves in Figs. 13 and 14 are obtained by multiplying the original HDDF values by the coefficients 1/2 for DPWM-C and 2/3 for DPWM-A, B, and D, taking SPWM as the basis.

VI. CONCLUSION

The harmonic distortion determining factor (HDDF), which represents the intrinsic spectral properties of PWM methods, is introduced. HDDF is almost independent of the inverter operating conditions such as the switching frequencies or load parameters if the switching frequency is 40 times greater than the output frequency. Furthermore, it has a close relation to the RMS values of the harmonic current and motor torque ripples for induction motor drives, or RMS values of the harmonic current and dc voltage ripples for rectifier operation. Therefore, it is useful as a common quality index for the evaluation of PWM methods.

Three typical analog PWM methods and four digital PWM methods are compared and evaluated based on HDDF values. It is shown that the harmonic injected PWM for analog PWM, or the digital PWM of type C have the best characteristics.

ACKNOWLEDGMENT

The authors wish to express their sincere appreciation to S. Sano, the former student, for his eager cooperation in completing this paper.

REFERENCES

- [1] R. Bonnert and R. Wu, "Improved three phase pulse width modulation for over modulation," in *Conf. Rec. 1984 IEEE Ind. Applicat. Soc. Ann. Meeting*.
- [2] J. Houldsworth and D. Grant, "The use of harmonic distortion to increase the output of a three-phase PWM inverter," *IEEE Trans. Ind. Applicat.*, vol. 20, no. 5, pp. 1224-1228, Sept./Oct. 1984.
- [3] T. Ohnishi and H. Okitsu, "A novel PWM technique for three phase inverter/converter," in *Conf. Rec. of 1983 IPEC-Tokyo*, pp. 384-395.
- [4] S. Fukuda, Y. Iwaji, and H. Hasegawa, "PWM technique for inverter with sinusoidal output current," *IEEE Trans. Power Electron.*, vol. 5, no. 1, pp. 54-61, Jan. 1990.
- [5] H. W. Van der Broeck, H.-Ch. Skudelny, and G. V. Stanke, "Analysis and realization of a pulsewidth modulator based on voltage space vectors," *IEEE Trans. Ind. Applicat.*, vol. 24, no. 1, pp. 142-150, Jan./Feb. 1988.
- [6] Y. Iwaji and S. Fukuda, "PWM waveform analysis using harmonic distortion determining factor for induction motor drives," in *Conf. Rec. 1991 IEEJ Hokkaido Branch Conv.*, pp. 72-73.
- [7] ———, "Waveform analysis of PWM inverters using the harmonic distortion determining factor," in *Conf. Rec. 1993 IEEJ National Conv.*, pp. 110-111.
- [8] ———, "A parameter designing method of PWM voltage source rectifier," *Trans. IEE J.*, vol. 112-D, no. 7, pp. 639-647, 1992.
- [9] ———, "PWM waveform analysis using harmonic distortion determining factor for voltage source rectifiers," in *Conf. Rec. 1991 IEEJ Hokkaido Branch Conv.*, pp. 74-75.
- [10] M. Boost and P. Ziogas, "State-of-the-art carrier PWM technique: A critical evaluation," *IEEE Trans. Ind. Applicat.*, vol. 24, no. 2, pp. 271-280, Mar./Apr. 1988.



Shoji Fukuda (M'85) received the B.E.E., M.S.F.E., and Ph.D. degrees from Hokkaido University, Sapporo, Japan, in 1965, 1967, and 1977, respectively.

In 1967, he joined the Faculty of Engineering, Hokkaido University, where he is currently an Associate Professor in the Department of Electrical Engineering. From 1981-1983, he worked at the University of Saskatchewan, Canada, as a postdoctoral fellow. He has been engaged in the research of microprocessor-based PWM control of

rectifiers/inverters, ac drives, and active power filters.



Yoshitaka Iwaji received the B.E.E. degree from Ibaraki University, Hitachi, Japan, in 1987, and the M.S.E.E. and Ph.D. degrees from Hokkaido University, Sapporo, Japan, in 1989 and 1992, respectively.

In 1992, he joined Hitachi Research Laboratory, Hitachi Ltd., Ibaraki, Japan, and has been engaged in research on PWM inverters for industrial applications.